

# Validation of X-in-the-Loop Approaches for Virtual Homologation of Automated Driving Functions

Stefan Riedmaier<sup>\*§</sup>, Jonas Nesensohn<sup>\*†</sup>, Christian Gutenkunst<sup>‡</sup>,  
Tobias Düser<sup>‡</sup>, Bernhard Schick<sup>\*</sup>, Housseem Abdellatif<sup>†</sup>

<sup>\*</sup>Kempen University of Applied Science, <sup>†</sup>TÜV SÜD Auto Service GmbH,  
<sup>‡</sup>AVL Deutschland GmbH, <sup>§</sup>Technical University Munich, Chair of Automotive Technology

**Abstract**—Securing and homologating automated driving functions presents a huge challenge for their market introduction due to an enormous number of scenarios and environment parameter combinations. Confronting conventional real world tests with the new challenges of automated driving is not feasible anymore and yields to a virtualization of the testing methods by means of X-in-the-Loop approaches. Since their validity is a key enabler for virtual homologation, this paper focuses on the validation of X-in-the-Loop approaches. A generic validation methodology is introduced and demonstrated for the specific use case of an automated longitudinal driving function. As a proof of concept equal scenarios are performed in real driving tests as reference and in two X-in-the-Loop approaches based on a test bed resp. a purely virtual co-simulation environment. The paper describes how a consistent implementation can be ensured to evaluate the collected data. First results show a promising correlation regarding multiple repetitions on the test bed and regarding the validation of both X-in-the-Loop approaches for a future virtual homologation of automated driving functions.

## I. MOTIVATION AND AIM OF WORK

Advanced Driver Assistance Systems (ADAS) in modern vehicles increase the safety by supporting the driver in his tasks. The systems are usually validated with field operational tests of about 1 million kilometers focusing to avoid false positives because the driver has to monitor the vehicle permanently [1]. The development towards automated driving would require even millions to billions of kilometers for a statistical prove against human accident databases according to [2]. There is consensus among experts: Mastering the effort in the future can only be achieved by means of significantly more simulation. Every test drive and every test kilometer are costly. To cope with increasing testing requirements virtualization is a promising method. Virtualized tests are cheap, time saving, reproducible and safety uncritical.

On the other hand, it is still unclear how safety-related functions for automated driving should be homologated. The experts agree on that it must come to a homologation directive. Virtual homologation will play a crucial role in this regard. Virtualization has even entered UN regulations for certification resp. homologation of vehicles by official authorities. Regulation 140 [3] for “approval of passenger cars with regard to Electronic Stability Control (ESC) Systems” explicitly allows simulation:

Where a vehicle has been physically tested in accordance with [...], the compliance of versions or vari-

ants of that same vehicle type may be demonstrated by a computer simulation [...].

The ESC homologation via Software-in-the-Loop (SiL) or Hardware-in-the-Loop (HiL) requires a vehicle dynamics model of sufficient quality to substitute the real vehicle. As a prerequisite for further simulations, the models must be validated against their real counterparts in different vehicle dynamics maneuvers.

In terms of automated driving, not only the demand for simulation is yet higher but also the complexity of X-in-the-Loop (XiL) approaches due to static and dynamic environmental influences, such as road environment and traffic scenarios. A consistent toolchain along the development and its validation will be a key enabler for securing and homologating automated driving. The question is now how can we qualify simulation environments and models for the homologation of automated driving functions? Can analogies to other areas be found here, even if the discipline of automatic driving is significantly more complex? Thus, this paper focusses on different XiL approaches and their validation against proving ground tests for the use case of an Automated Longitudinal Driving (ALD) function.

## II. STATE OF THE ART

### A. X-IN-THE-LOOP METHOD

The time-tested V-Process continues to provide the framework in vehicle development. In view of the complexity of today’s and future testing and integration tasks, all components have to be included and validated in the entire evaluation process as early as possible in an approach known as front loading. To do so, the traditional V-Process of the individual domains is interlinked with and decomposed into relevant mini V-Processes. The integration work across several domains is performed at a very early stage in the whole virtual vehicle using the XiL method [4]. It allows the interactions and correlations of interaction chains to be evaluated very early and corrected immediately if required. Agile system development that is consistently focused on the behavior of the whole vehicle is thus made possible.

XiL in this context stands for the seamless integration of all relevant components and systems – software, hardware, model – in the development, integration and test loops. Due to

virtual integration in the context of the V-Model it is possible to know at any time what effects the tested component has on the overall system, the whole vehicle or driving properties, for example. Consequently, interactions can be detected in an early concept phase and appropriate actions taken to avoid costly errors and time loss. In addition to virtual integration, seamless and standardized whole vehicle evaluation in cross-functional maneuver catalogs plays a central role. Knowing at any time what contribution a component has on the overall driving properties and being able to compare the results between road test, rig test and simulation marks a major step forward in terms of quality and efficiency.

In the field of powertrain development, more and more, a powertrain or full-vehicle test rig is being used as Vehicle-Hardware-in-the-Loop (VHiL) approach [5] between the classic HiL test and road test (Figure 1). Here, everything that does not exist as hardware is simulated as a so-called residual vehicle or the residual environment. This makes it possible to realistically validate the entire vehicle in real driving maneuvers or driving scenarios. This provides more certainty whether the functions in the overall system run as desired. In addition, it provides the possibility of faster commissioning and easier and reproducible troubleshooting if errors occur on the real road. It is very interesting, if such a XiL test method can also be used for automated driven vehicles, which will be discussed in more detail in the following paper.

Another test approach according to the state of the art is the so-called Vehicle-in-the-Loop (ViL) method, which is not shown in Figure 1. Here, too, the residual of the vehicle or the residual of the environment is simulated. This means that traffic scenarios, road infrastructure and environment sensors are simulated. The sensor signals are fed as object lists or camera images into the real Electronic Control Units (ECUs) via a bypass. The vehicle moves on an open-air site such as a vehicle dynamics platform or a defined environment on the proving ground [6].

## B. VALIDATION METHODS

The UN/ECE-R 140 [3] does not provide a clear specification and recommendation for the subsystem models, on the method, the maneuvers and the evaluation criteria to validate the simulation tools. The directive enables the technical service, in cooperation with the vehicle manufacturers and suppliers, to create an appropriate procedure based on their own expert knowledge. Unfortunately, the directive did not have any preexisting standards for the validation of simulation tools. In order to keep the interpretations as low as possible and to achieve more safety during a homologation process, the German standardization committee has launched national and international activities at an early stage to develop a uniform standard. Extensive preliminary analysis of various driving maneuvers led to two key maneuvers for the UN/ECE-R 140 [3], in which the quality assessment of the simulation can be carried out by means of certain characteristic parameters. These were then developed at the national and international level in close cooperation between the international vehicle

industry and research institutes. At the end, stationary and transient validation maneuvers, characteristic values and tolerances were selected, which can adequately ensure the quality of the simulation in the specific driving maneuvers [7].

Therefore, a two level validation approach was selected. At first the validation of the passive vehicle (without ESC controller) has to be performed according to ISO 19364 [8] within the steady-state circular driving maneuvers. Values of lateral acceleration, steering wheel angle, sideslip angle, and roll angle from physical testing shall be obtained as specified in ISO 4138 [9] or the Slowly Increasing Steer Test [10] and plotted along with the boundaries obtained from the simulation. Figure 2a shows the validation approach with top and bottom boundaries for a vehicle with limit understeer behavior. In Figure 2a, several ovals are used to group top and bottom boundary points, indicated with circular markers, with the corresponding point from the simulation, indicated with a plus marker. Offsets and gains as related tolerances  $\epsilon_x$  and  $\epsilon_y$  can be defined accordingly [8].

Secondly, the validation of the active vehicle (with ESC controller) has to be performed according to ISO 19365 [10] within the transient Sine-with-Dwell maneuver, which is required for the UN/ECE-R 140. The simulation and physical test results are compared on the basis of characteristic values of variables recorded at the specific conditions according to Figure 2b. Tolerances allowed between metrics obtained from physical testing and simulation can be defined based on the given characteristic values.

In the meantime, several more simulation and validation standards are being developed within the ISO/TC 22/SC 33/WG 16 working group.

- 1) ISO Comment Draft 19585:  
Heavy commercial vehicles and buses – Vehicle dynamics simulation and validation – Steady-state circular driving behavior [11]
- 2) ISO Comment Draft 19586:  
Heavy commercial vehicles and buses – Vehicle dynamics simulation and validation – Dynamic lateral stability of vehicle combinations [11]
- 3) ISO Preliminary Work Item 22135:  
Heavy commercial vehicles and buses – Calculation for steady state roll-over threshold [11]
- 4) ISO Preliminary Work Item 21233:  
Heavy commercial vehicles and buses – Vehicle dynamics simulation and validation standard – Closing curve test [11]
- 5) ISO Preliminary Work Item 22140:  
Passenger cars – Validation of vehicle dynamics simulation – Lateral transient response test methods [11]

An ISO Preliminary Work Item is still under development. An ISO Comment Draft has been submitted to the various member countries to comment on an standard draft. The validation approaches of the mentioned standards above are almost the same as the ISO 19364/19365 even with specific applications.

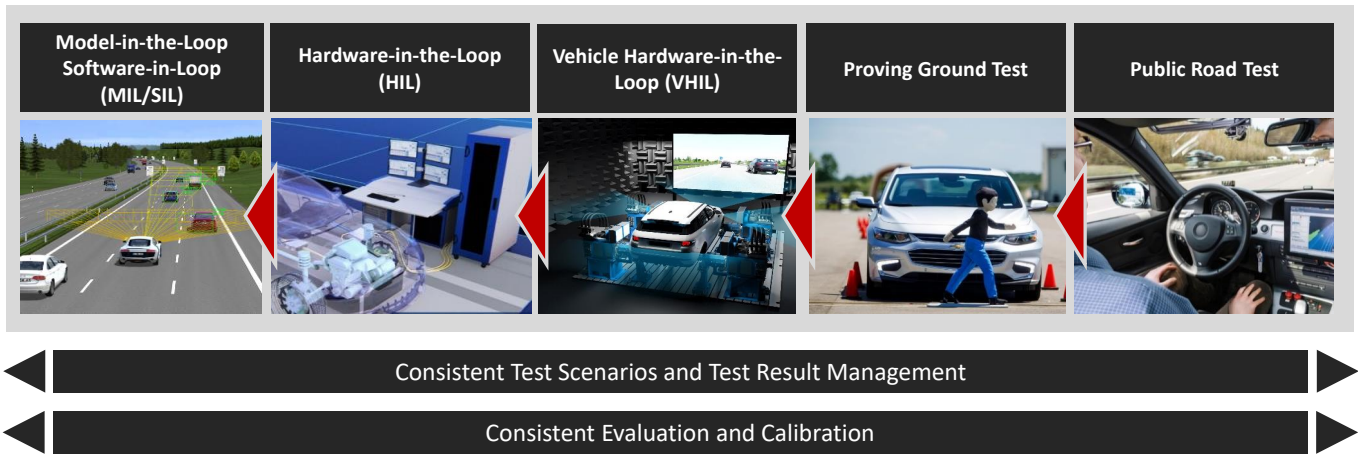


Fig. 1: Consistent test instances based on XiL approaches

### III. GENERIC METHODOLOGY FOR VALIDATION OF X-IN-THE-LOOP APPROACHES

This section introduces a methodology how to validate XiL approaches compared to real driving tests. The XiL validation architecture is visualized in the block diagram in Figure 3. Each test instance is simplified to one line in the diagram following the processing chain Sensor-Function-Vehicle. Different sensors perceive the environment – consisting of static scenery and dynamic traffic objects of a scenario. The sensors provide the Automated Driving (AD) function with their environment information. The AD function calculates control signals for the actuators in the vehicle so that the resulting vehicle dynamics follows the desired behavior. For clarity, loops back from the vehicle as well as an additional driver block are omitted in Figure 3. For automated vehicles, the human driver is still in the loop and especially relevant for transition test cases. However, as the automated vehicle itself and not the driver shall be secured and homologated in the future, the driver is here not the focus for the validation of XiL approaches.

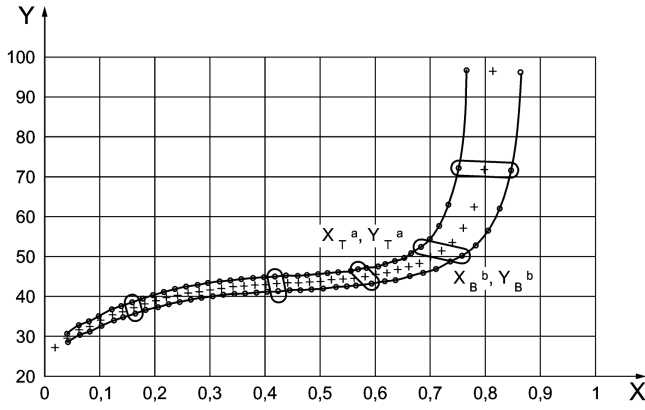
The top line in Figure 3 includes the real driving tests as reference for comparison. Each single XiL approach is realized as one further line with increasing virtualization from top to bottom. For SiL resp. MiL the whole processing chain is virtual, for HiL the AD function is integrated as real component and for ViL resp. VHiL the AD function and the vehicle [12]. It should be noted that it is also possible to replace the virtual sensor model by physical stimulation of the real sensor [13]. To validate XiL approaches against real driving tests by comparing result signals, all test instances have to get the exact same input signals ( $\Rightarrow$ ). Then good simulation models that fit their real counterparts in the same column in Figure 3 will lead to similar behavior as in reality. Bad simulation models will cause big differences ( $\Delta$ ) between the result signals and hurt certain tolerances.

### IV. USE CASE OF AUTOMATED LONGITUDINAL DRIVING

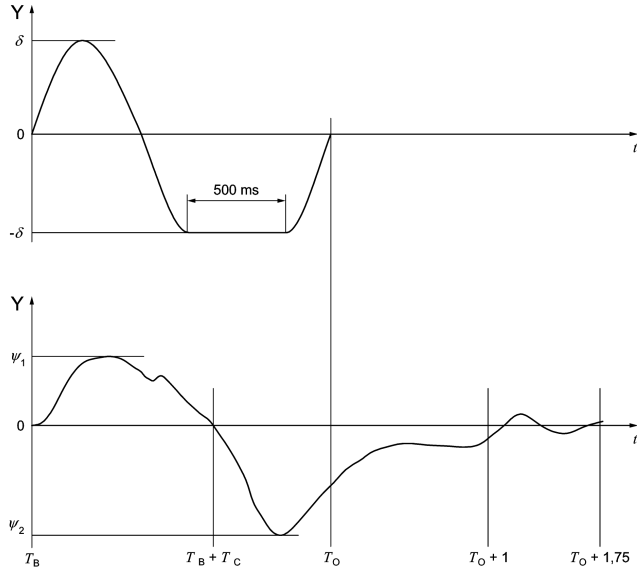
#### A. SPECIFIC USE CASE METHODOLOGY

The further sections focus on the validation of the VHiL and MiL approaches in the use case of an Automated Longitudinal Driving (ALD) function as a proof of concept. Therefore the specific methodology – visualized in Figure 4 – is derived from the generic methodology of Section III. Since the paper is dedicated to the validation of XiL approaches for homologation of automated driving functions, the focus is on the function itself. It has to be considered as a unit together with the vehicle to close the control loop. Validating sensor models can be separated and is not realized in this paper as well as to complete the Sensor-Function-Vehicle chain. It will be part of the authors' future work. Thus, the unit of function and vehicle enables exploiting the analogy of the two-stage validation process introduced in Section II-B. There the passive vehicle model must be validated at first for steady-state circular driving according to ISO 19364 [8] before the influence of the ESC controller can be added for Sine-with-Dwell tests in ISO 19365 [10].

In the first step of the two-stage process, a KIA Soul is selected as the Vehicle Under Test (VUT). As no vehicle dynamics model of the KIA Soul was available, the validation of the passive vehicle model had to be replaced by its parametrization and tuning in Section IV-B. This was executed based on own static and longitudinal dynamic measurements. After an initial parametrization, the model was tuned until it reached a valid stage. In the second step, an ALD function (see Section IV-C) was added to the vehicle dynamics for the use case of automated longitudinal driving. To focus on the unit of function and vehicle, a test driver is required that bypasses the actual sensor, provides the ALD function with the necessary input signals and stores the relevant output signals. The realization of the test driver via Vehicle-to-Vehicle Communication by means of Inertial Measurement



(a)



(b)

Fig. 2: (a) Validation method based on boundaries, (b) Validation method based on characteristic values

(a) Key: Lateral acceleration ( $X$ ), boundaries for steering wheel angle ( $Y$ ), top boundary points ( $X_{T^a}, Y_{T^a}$ ), bottom boundary points ( $X_{B^b}, Y_{B^b}$ ),

(b) Beginning of Steer – BOS ( $T_B$ ); Competition of Steer – COS ( $T_O$ ); Zero crossing for yaw rate ( $T_B + T_C$ ); yaw rate at 1 s after COS ( $T_O + 1$ ); yaw rate at 1.75 s after COS ( $T_O + 1.75$ )

Units (IMUs) in the real world and via ideal sensors in the virtual world is described in Section V.

The prerequisite to provide same input signals ( $=$ ) in Figure 4 can be achieved by starting with real driving tests on the Proving Ground (PG), measuring the dynamic ground truth for the ALD function with precise IMUs and generate therefrom virtual scenarios without any modifications. After executing the tests, Key Performance Indicators (KPIs) can be calculated and compared ( $\Delta$ ) between the VHiL resp. MiL approach and the PG tests. The KPI analysis is performed

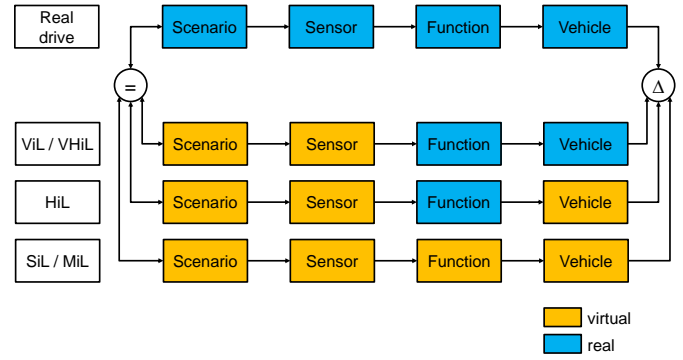


Fig. 3: Generic methodology for validation of XiL approaches

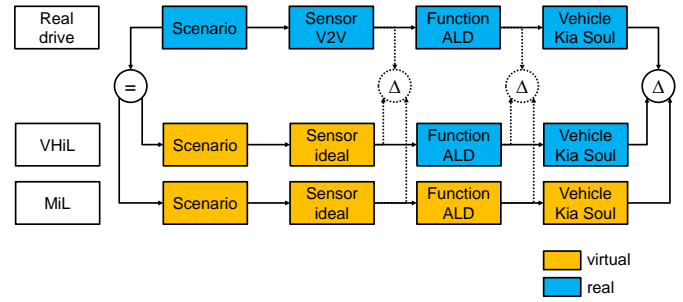


Fig. 4: Specific use case methodology.  
V2V = Vehicle-to-Vehicle Communication

at different levels of the processing chain. The comparison takes place evaluating the vehicle dynamics complemented with some input and output ALD signals.

## B. VEHICLE MODEL PARAMETRIZATION

To get a good comparison between the MiL approach and real driving tests, a vehicle dynamics model of the Vehicle Under Test (VUT) needs to be parametrized. Traffic Simulation Vehicles (TSVs) surrounding the VUT do not require any vehicle dynamics model at all, because measurements from the test track will be imported directly as driven trajectory into the simulation. The generation of the vehicle dynamics model of the VUT is split in an initial parametrization followed by an iterative fine-tuning until the model is valid.

Due to the use case of ALD, no fully parametrized vehicle model with all subcomponents is required. For longitudinal dynamics the stabilizer, suspension kinematics and steering can be neglected. Regarding the relevant subcomponents, a few of the main parameters like wheelbase, tires, gearbox and power map are even open accessible and directly used for the initial parametrization. Other parameters like vehicle mass and center of gravity are determined by static measurements according to ISO 10392 [14] with the complete measurement hardware. To ensure autonomy between the vehicle model parametrization and the later validation of the XiL approaches completely separate dynamic measurements without the ALD function are performed here. The power curve is measured on a chassis dynamometer, the driving resistance with dynamic

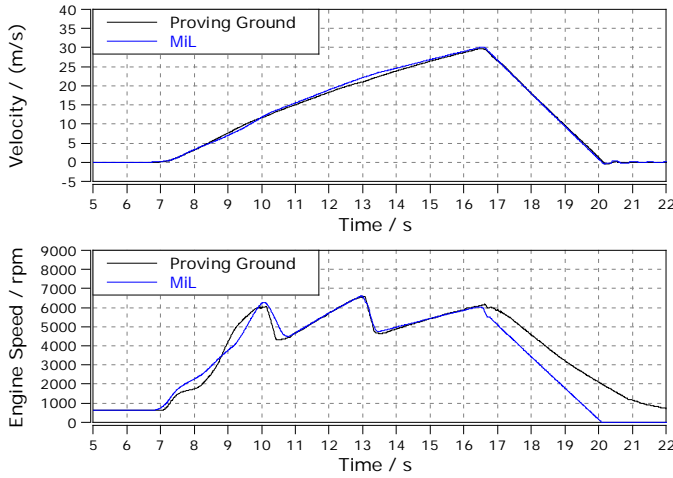


Fig. 5: Passive vehicle model tuning based on full acceleration and full braking

coast down on a test track. Additionally, longitudinal dynamic tests with different scales of throttle and brake up to full acceleration and full braking are executed. To parametrize a hydraulic brake model comparisons between brake pedal force resp. position, brake pressure and deceleration are made.

The data from the longitudinal dynamics tests is used for the iterative fine-tuning until the model is valid. This is illustrated in Figure 5 by means of the full acceleration and braking maneuvers. Velocity and engine speed are two important signals to reveal performance differences in the physical structure of the vehicle model. As this paper is focused on the validation and not on model development a trade-off between parametrization effort and perfect model validity had to be found. Latencies, pedal maps, efficiencies, torque build-up, turbo charger characteristics and shift strategy are not modelled. Anyway, the final state in Figure 5 manifests sufficient validity for our proof of concept.

### C. AUTOMATED LONGITUDINAL DRIVING FUNCTION

Since the focus of this paper was on the comparison of different XiL approaches and not on the evaluation of the automated driving function it was necessary to have a white box model of the function. Only if this is ensured, the controller can be used in the real VUT on a rapid prototyping ECU and as a model in the simulation of the virtual VUT. For that reason, a simple self-developed ALD controller was used.

The ALD consists out of two different control strategies. The first one is the distance control, which takes care, that the VUT follows a TSV within a defined time gap. If there is no TSV in front of the VUT the speed control is active and ensures that the set speed is held. Both control strategies calculate a desired acceleration within the limits defined in [15], which is converted in throttle ( $\alpha$ ) and brake pedal position ( $s_b$ ). With these signals, the VUT is controlled.

## V. IMPLEMENTATION OF THE VALIDATION METHODOLOGY

### A. PROVING GROUND TESTS

The setup of the real driving tests on the Proving Ground (PG) is illustrated in Figure 6. The VUT and TSV are both equipped with precise measurement systems to locate their position accurately. These IMUs perform their calculations based on GPS and GLONASS satellites and a real-time kinematic system that is powered over the mobile phone network. Their data is used to bypass the actual environment sensor and to provide the ALD function with the necessary input signals. These include the absolute velocity and acceleration of the VUT as well as the relative velocity and the relative distance in longitudinal and lateral direction. Whereas the absolute signals are fed directly into the ALD function, for the relative signals a Vehicle-to-Vehicle Communication is established over a Wi-Fi network with directional antennas. Both the absolute and the relative signals are measured in the vehicle-based coordinate system of the VUT in accordance with [16]. The IMUs offer the possibility to transfer the origin of the coordinate system from the antenna to specific point of interests. For the use case of ALD, the VUT's reference point is placed on the front and the TSV's reference point on its rearmost edge. This simplifies the setup because the IMU of the VUT calculates directly the appropriate signals for the ALD function and no further processing is required.

To send the IMU data to the ALD function, a separate Controller Area Network (CAN) bus for vehicle control is integrated in the VUT. The connection of the ALD function to the CAN bus is realized with the rapid prototyping ECU in Figure 6. The latter executes the ALD function from Section IV-C compiled for the specific target. The ALD function calculates the desired throttle and brake commands. To forward them from the rapid prototyping ECU to the VUT, an external car control for brake and acceleration is required as vehicle interface. To control the braking system of the VUT a braking robot is installed and also connected to the separate vehicle control CAN bus. Based on brake commands of the ALD function a position controlling system actuates the braking robot to the desired position ( $s_b$ ).

To control the accelerator pedal an additional interface module is required. This module controls the accelerator pedal by calculating spoofed sensor voltages. Two sensors are integrated in the pedal actuator to measure the pedal position. The module is connected via a Y joint to the accelerator pedal and the engine ECU. The interface receives target values for the position over CAN and converts this information to output voltages which are simulating a driver input. If no action is send to the module, all acceleration pedal inputs are passed through the interface directly to the engine ECU. To reduce the complexity of the actuation a car with dual clutch transmission (automatic transmission) is used to avoid the installation of a clutch and shifting robot.

Furthermore, the data of both IMUs is not just used for online PG tests, but also stored for the import of the real

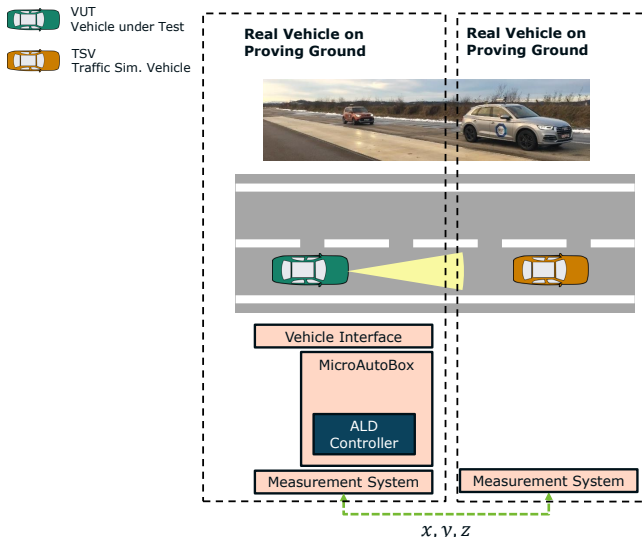


Fig. 6: Overview of Proving Ground topology

scenarios into the virtual world in Section V-B and Section V-C and finally for data evaluation in Section VI.

### B. VEHICLE-HARDWARE-IN-THE-LOOP AS DRIVINGCUBE CONFIGURATION

The VHiL approach is realized by means of an AVL DRIVINGCUBE™ configuration [17] that builds up on an AVL ROADSIM™ Chassis Dynamometer with additional hardware and software specific for the ADAS/AD application, such as sensor and environment simulation. For the use case of ALD, the implemented toolchain includes an extended vehicle, environment and traffic simulation and the interface to the ALD function of the VUT. With this upgrade, the Chassis Dynamometer is capable to even validate and optimize ADAS/AD functions and to transfer certain scenarios and maneuvers from the proving ground to the chassis dynamometer. To emphasize both the generic VHiL method and the implementation as DrivingCube configuration the consistent terminology VHiL/DrivingCube is used in the remaining paper.

The measured data of the TSV from Section V-A is integrated in the co-simulation platform Model.CONNECT™ in Figure 7 as a signal table and transferred to the environment simulation VIREs Virtual Test Drive to re-simulate the exact testing conditions from the PG. To achieve this the VUT and TSV are placed in the environment simulation on the same starting positions as their counterparts from the PG tests. Subsequently the virtual TSV drives the same trajectory as the real TSV so that the equal testing conditions exist for the unit of function and VUT. Thanks to this consistency, it will be possible later to compare the VHiL/DrivingCube and the MiL approach to the PG tests. To detect the TSV in the simulation an ideal sensor is mounted on the simulated VUT. This sensor provides the signals for delta distance ( $\Delta s$ ), delta velocity ( $\Delta v$ ) and the lateral distance, which is used to determine if the TSV is a relevant target. The target is classified as

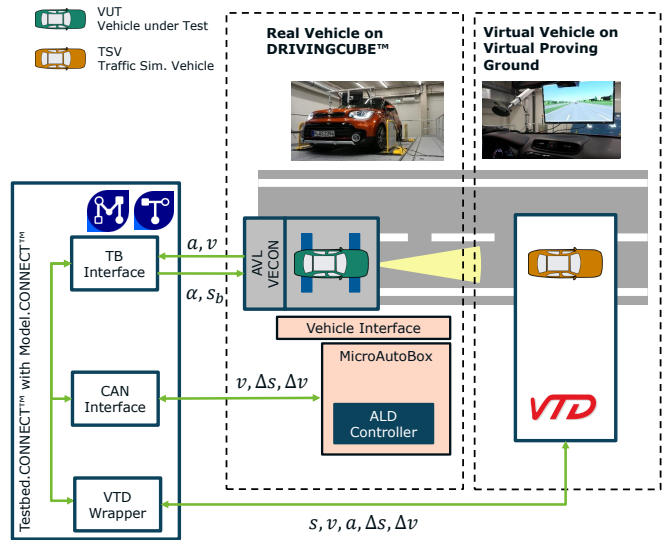


Fig. 7: Overview of VHiL/DrivingCube configuration

relevant, if the lateral distance is below a certain value. The environment simulation delivers this information via a local area network connection to the co-simulation platform. From there the information is sent to the vehicle control CAN bus introduced in Section V-A.

The signals for actual speed ( $v$ ) and acceleration ( $a$ ) of the VUT are provided by the chassis dynamometer via test bed CAN to the simulation. From there the information is forwarded to the environment simulation to move the ego vehicle. The signals are also forwarded to the vehicle control CAN where the rapid prototyping ECU is connected and uses these signals to calculate the desired throttle and brake commands. Resulting out of the throttle and brake commands the real VUT generates a tractive force on the test bed that finally results in a rotational speed of the chassis dynamometer.

That means that the real VUT gets the same signals on the same CAN identifier for the VHiL/DrivingCube test runs as for the PG tests.

### C. MODEL-IN-THE-LOOP

For the MiL approach in Figure 8, the virtual part of the VHiL/DrivingCube approach can be reused completely. As described in Section V-B, the real measurement data is imported via signal table, sent to the environment simulation where an ideal sensor recognizes the relevant traffic object and provides the signals for distance ( $\Delta s$ ) and relative velocity ( $\Delta v$ ). The ideal sensor routes the environment signals to the ALD function without any modifications.

The MiL approach replaces the real function and vehicle by the ALD model from Section IV-C and the vehicle dynamics model from Section IV-B. The ALD function is identical for real and virtual test instances, just compiled for different targets. Whereas the target for tests with real function is the rapid prototyping ECU, for MiL the ALD function was compiled as Functional-Mockup-Unit. The Functional-Mockup-Unit takes

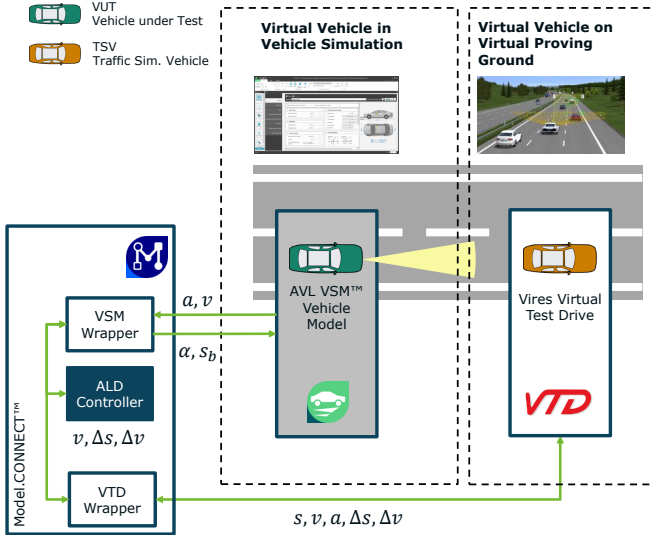


Fig. 8: Overview of MiL topology

the distance ( $\Delta s$ ) and relative velocity ( $\Delta v$ ) from the ideal sensor and calculates desired throttle and brake commands for the vehicle dynamics model. The latter determines the vehicle movement, feeds back the new actual speed ( $v$ ) and acceleration ( $a$ ) into the ALD function and exchanges query points and vehicle dynamics with the environment simulation. To sum up, the MiL approach is executed in the same co-simulation platform, which integrates and connects all its models, as in Section V-B.

## VI. SCENARIOS AND DATA EVALUATION

### A. SCENARIO DESCRIPTION

For the validation of the XiL approaches in the use case of ALD four scenarios were defined in Table I.

### B. REPEATABILITY OF VEHICLE-HARDWARE-IN-THE-LOOP / DRIVINGCUBE

The first step for validating VHiL/DrivingCube and MiL against the PG tests is to show that the VHiL/DrivingCube test runs are reproducible after import of the real scenarios into the virtual world. For the MiL approach this is ensured, anyway. To verify this each PG scenario was repeated five times on the VHiL/DrivingCube. The results are shown in this subsection using the example of all five repetitions of scenario 2.

At first the initial values for delta distance ( $\Delta s$ ), velocity ( $v$ ), acceleration ( $a$ ) and velocity of TSV ( $v_{TSV}$ ) are compared for each scenario. The initial values of scenario 2 are shown in Table II and match almost perfectly after the scenario import.

Then the plots over time are compared for the five repetitions in Figure 9. The velocities of the imported TSV ( $v_{TSV}$ ) coincide in Figure 9a. The comparison takes places at different levels of the processing chain Sensor-Function-Vehicle. Delta velocity ( $\Delta v$ ) (see Figure 9b) and delta distance ( $\Delta s_{act}$ ) (see Figure 9c) are input signals of the ALD function, the desired acceleration ( $a_{des}$ ) (see Figure 9d) is calculated by the ALD

function and the VUT velocity ( $v$ ) (see Figure 9e) is part of the vehicle dynamics. The upper and lower limit in Figure 9e is calculated according to [18] annex 7: “tolerances on speed ( $\pm 2$  km/h) and on time ( $\pm 1$  s) are geometrically combined at each point”.

Beside the validation method based on plots and boundaries (see Section II-B), for the validation method based on characteristic values the following Key Performance Indicators (KPIs) are defined. The first and second KPIs are the average (see Equation 2) and the maximum (see Equation 3) of the standard deviation for the five repetitions over time.

$$\sigma(t) = \sqrt{\frac{\sum_{i=1}^n (x_i(t) - \bar{x}(t))^2}{n-1}} \quad (1)$$

$$\hat{\sigma} = \max \sigma(t) \quad (2)$$

$$\bar{\sigma} = \frac{1}{n} \sum_{t=1}^T \sigma_t \quad (3)$$

The relation between maximum and average value shows if the signal has a constant high deviation ( $\bar{\sigma} \approx \hat{\sigma}$ ) or has only one or more peaks ( $\bar{\sigma} \ll \hat{\sigma}$ ).

The next KPI is the correlation between the repetitions. The correlation is calculated as shown in Equation 4.

$$r = \frac{s_{xy}}{s_x s_y} = \frac{\sum_{t=1}^T (x_t - \bar{x})(y_t - \bar{y})}{\sqrt{\sum_{t=1}^T (x_t - \bar{x})^2 \sum_{t=1}^T (y_t - \bar{y})^2}} \quad (4)$$

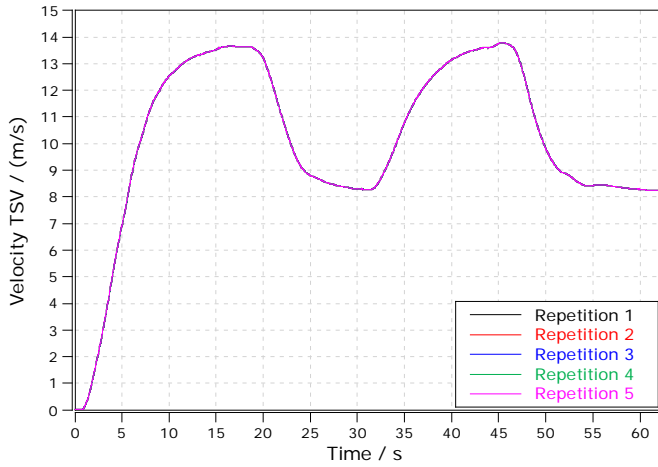
To be sure, that the correlation does not only fit the curve shape but also the scaling the average value is taken into account. The average value can be calculated as shown below (see Equation 5).

$$\bar{x} = \frac{1}{n} \sum_{i=1}^n x_i \quad (5)$$

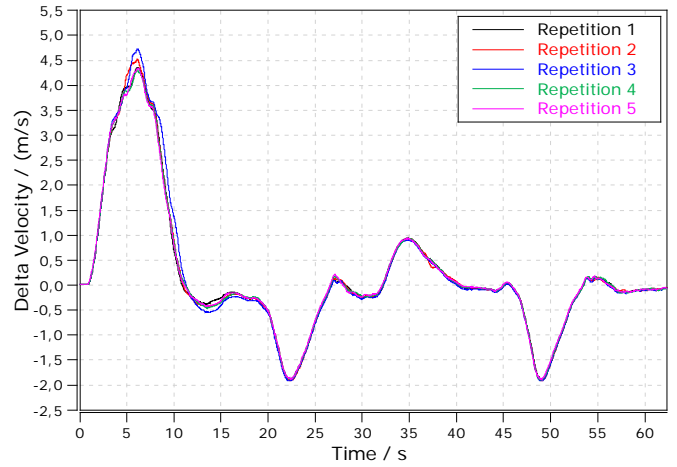
The first two KPIs have been calculated for the same signals as plotted in Figure 9 and are shown in Table III. The correlation of the VUT velocity between the repetitions is shown in Table IV and is very good. The average velocity is also shown in Table V.

It should be noted that the vehicle has an automatic transmission and was in D mode. This means that the gear changes are not influenced by the test bed control or operator and vary between the five repetitions. Because of that, the vehicle also showed a different acceleration behavior, which explains the deviation of the delta distance. Especially in repetition 3 of Figure 9 this behavior can be seen. To restrict this variation in a future test run the manual shifting mode will be used and controlled by the test bed control or operator.

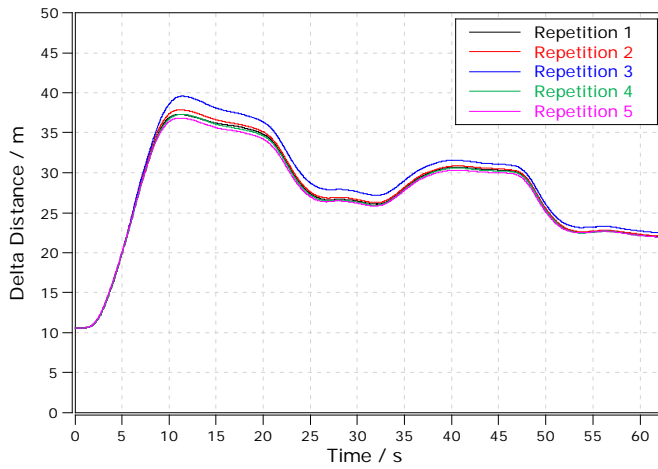
For the other three proving ground scenarios, the results are similar to the shown ones for scenario 2. For the higher speed scenarios, the standard deviation for delta distance, delta velocity and VUT velocity is a bit higher, but remains within the same range in percentage.



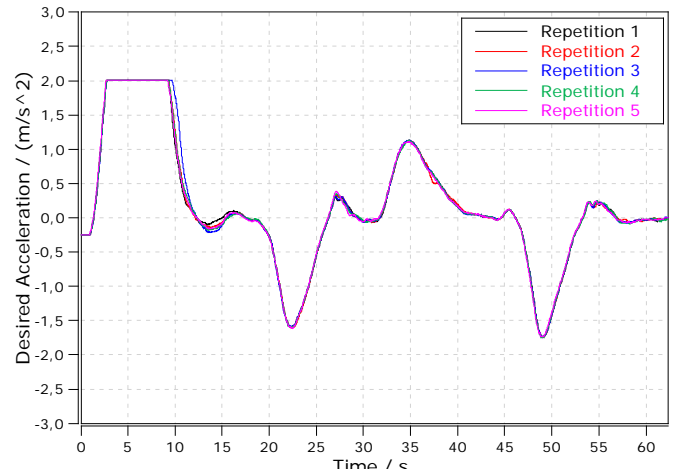
(a)



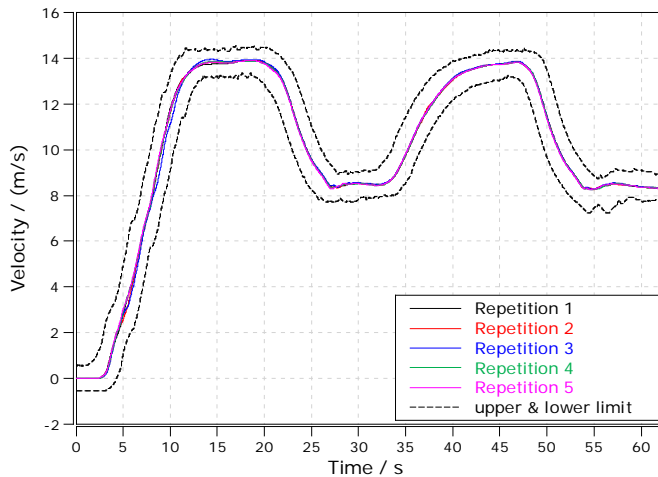
(b)



(c)

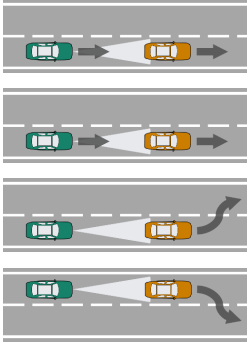


(d)



(e)

Fig. 9: Comparison of the VHiL/DrivingCube repetitions by means of (a) TSV velocity, (b) delta velocity, (c) delta distance, (d) desired acceleration and (e) VUT velocity.



**Scenario 1:**

From standstill follow-up with 50 km/h reducing to 30 km/h back up to 50 km/h and 30 km/h again

**Scenario 2:**

From standstill follow-up with 80 km/h reducing to 60 km/h back up to 80 km/h

**Scenario 3:**

From standstill follow up with 60 km/h, TSV pull out left, VUT accelerate to 80 km/h

**Scenario 4:**

From standstill follow up with 60 km/h, TSV pull out right, VUT accelerate to 80 km/h

TABLE I: Scenario description

Repetition	$\Delta s/$ m	$v/$ (m/s)	$a/$ (m/s <sup>2</sup> )	$v_{TSV}/$ (m/s)
#1	10,592	-0,001	0,000	0,015
#2	10,592	0,000	0,000	0,015
#3	10,592	0,000	0,000	0,015
#4	10,592	0,000	0,000	0,015
#5	10,592	0,000	-0,001	0,015

TABLE II: Initial values for the VHiL/DrivingCube repetitions

	$v_{TSV}/$ (m/s)	$\Delta v/$ (m/s)	$\Delta s_{act}/$ m	$a_{des}/$ (m/s <sup>2</sup> )	$v/$ (m/s)
$\bar{\sigma}$	0,003	0,039	0,496	0,020	0,041
$\hat{\sigma}$	0,010	0,283	1,082	0,257	0,324

TABLE III: Mean and maximum standard deviation for the five VHiL/DrivingCube repetitions

C. COMPARISON OF THE THREE TEST INSTANCES

The comparison of the three test instances PG, VHiL/DrivingCube and MiL is done consistently with the same scenario and the same two validation methods based on plots and boundaries and based on characteristic values as already used in Section VI-B.

	#1	#2	#3	#4	#5
#1	1	0,9999	0,9994	0,9999	0,9999
#2	0,9999	1	0,9995	0,9999	0,9998
#3	0,9994	0,9995	1	0,9994	0,9992
#4	0,9999	0,9999	0,9994	1	0,9992
#5	0,9999	0,9998	0,9992	0,9992	1

TABLE IV: Correlation of the VHiL/DrivingCube repetitions

	#1	#2	#3	#4	#5
$\bar{v}/$ (m/s)	10,0078	10,0064	10,0000	10,0086	10,0103

TABLE V: Average of the VHiL/DrivingCube repetitions

	$\Delta s/$ m	$v/$ (m/s)	$a/$ (m/s <sup>2</sup> )	$v_{TSV}/$ (m/s)
PG	10,586	0,000	0,0022	0,015
VHiL/DC	10,592	-0,001	0,0002	0,015
MiL	10,591	0,000	0,0000	0,015

TABLE VI: Initial values of the three test instances

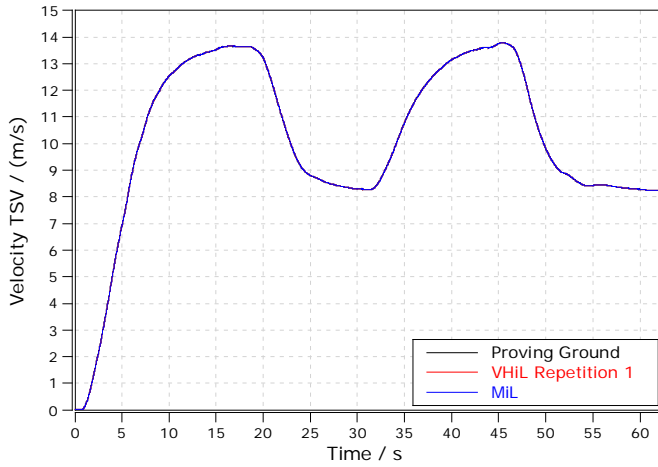
	$v_{TSV}/$ (m/s)	$\Delta v/$ (m/s)	$\Delta s_{act}/$ m	$a_{des}/$ (m/s <sup>2</sup> )	$v/$ (m/s)
$\bar{\sigma}_{VP}$	0,0035	0,0668	0,2413	0,0592	0,0716
$\hat{\sigma}_{VP}$	0,0253	0,4097	0,8058	0,4190	0,4174
$\bar{\sigma}_{MP}$	0,0035	0,1301	0,5938	0,1040	0,1365
$\hat{\sigma}_{MP}$	0,0253	0,5292	1,4623	0,5554	0,5683

TABLE VII: Mean and maximum standard deviation of VHiL/DrivingCube and PG ( $\bar{\sigma}_{VP}$  and  $\hat{\sigma}_{VP}$ ) resp. MiL and PG ( $\bar{\sigma}_{MP}$  and  $\hat{\sigma}_{MP}$ )

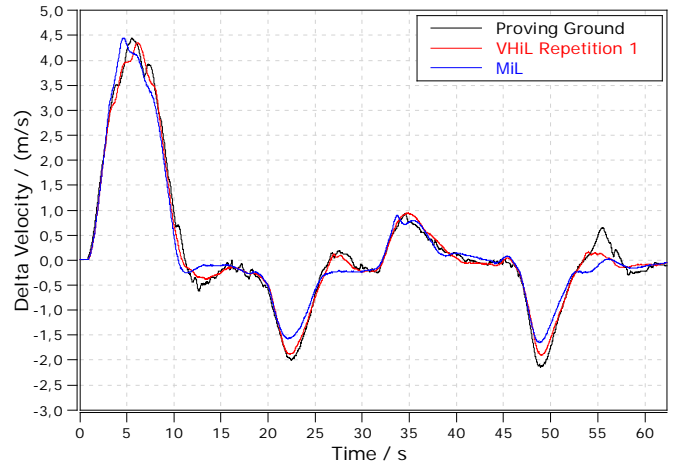
The initial values for delta distance ( $\Delta s$ ), velocity ( $v$ ), acceleration ( $a$ ) and velocity of TSV ( $v_{TSV}$ ) are shown in Table VI. Beside the initial values that match very well the curves over time are shown in Figure 10 for velocity of TSV ( $v_{TSV}$ ), delta velocity ( $\Delta v$ ), delta distance ( $\Delta s_{act}$ ), desired acceleration ( $a_{des}$ ) and VUT velocity ( $v$ ). The curves over time look similar for the three test instances. Proving ground and VHiL/DrivingCube match very well, MiL has a little more deviation compared to the proving ground, but still lies within the boundary in Figure 10e. The first two KPIs (see Section VI-B) for the validation of VHiL/DrivingCube and MiL against the PG tests are shown in Table VII. For the three test instances, a correlation is calculated as defined in Equation 4 and can be seen in Table VIII.

	PG	VHiL/DC	MiL
PG	1	0,9994	0,9974
VHiL/DC	0,9994	1	0,9980
MiL	0,9974	0,9980	1

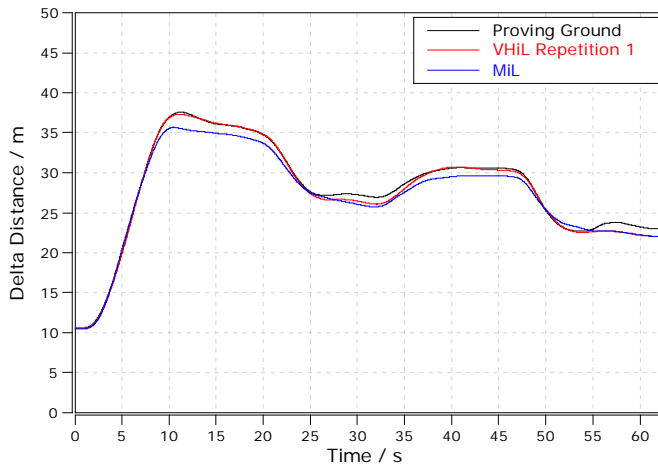
TABLE VIII: Correlation of the three test instances



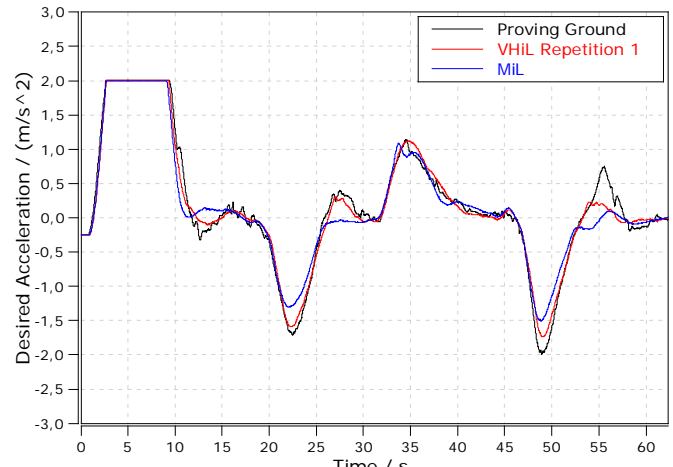
(a)



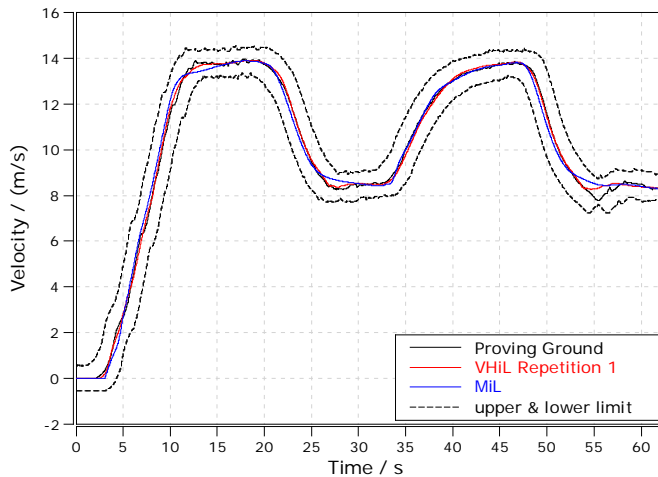
(b)



(c)



(d)



(e)

Fig. 10: Comparison of the three test instances by means of a) TSV velocity, b) delta velocity, c) delta distance, d) desired acceleration and (e) VUT velocity.

The comparison of proving ground and VHiL/DrivingCube matches very well for all driven scenarios. The standard deviation is always relatively low and the correlation very high. For the comparison between proving ground and MiL a slightly higher deviation can be seen. This deviation results from the modeling quality. Latencies, pedal maps, efficiencies, torque build-up, turbo charger characteristics and shift strategy were not modelled in the first step. Whereas the passive vehicle matched well in Section IV-B, the additional braking robot, latencies and pedal maps were identified as the sources of deviation. To sum up, first results for the validation of VHiL/DrivingCube and MiL compared to PG tests in four scenarios of the ALD use case show promising results. This work will be extended for further scenarios and evaluations in the future.

## VII. CONCLUSION

It's a changing world! Advanced Driver Assistance Systems and Automated Driving shall provide more comfort, time and safety. Perceptions and decision made by the driver today will be made by ADAS/AD functions in the future. The driver will be driven.

To achieve this target a lot of new technologies and functions have to be developed, integrated and connected in the vehicle. The complexity increases tremendous with related consequences on validation and homologation.

This paper introduced a new method for the validation of XiL approaches that can also be used for the virtual homologation of Automated Driving Functions. In addition to the proving ground, homologation tests can be shifted to empowered VHiL test beds as well as MiL/SiL/HiL simulation environments. The key is the seamless toolchain and a comparability between the different test instances. Based on that the homologation process can be optimized by a scenario- and test case-oriented combination of the proving ground, DrivingCube and MiL/SiL/HiL approach to use the benefits of each test instance.

Based on four different scenarios a proof of concept was executed and introduced in this paper. The good correlation between the three test instances could be shown. Beyond the development of new tools and new methods the certification of those to use them for homologation is always a challenge. That topic was considered as the Chassis Dynamometer is already used for emission homologation and the simulation approaches for ESC homologation in comparable way. This laid an important foundation that will be improved in upcoming steps.

## ACKNOWLEDGMENT

The research presented was conducted in cooperation with TÜV SÜD Auto Service GmbH and AVL Deutschland GmbH. The authors would like to thank AVL Zöllner GmbH for providing the AVL ROADSIM™ Chassis Dynamometer and Rolf Hettel<sup>‡</sup> for accompanying the DrivingCube tests. Further thanks to Benjamin Koller<sup>†</sup> and Frank Diermeyer<sup>§</sup> for supporting the research project as well as to Christian Gnad<sup>†</sup>,

Thomas Ponn<sup>§</sup> and Markus Lienkamp<sup>§</sup> for feedback regarding the paper.

## CONTRIBUTION

Stefan Riedmaier is the initiator and main author of this paper. He contributed the methodology and accompanied the whole research. Stefan Riedmaier created the virtual world from the real measurement data for the DrivingCube and Model-in-the-Loop approaches and performed the simulations. Jonas Nesensohn is primarily responsible for the proving ground tests and vehicle model parametrization. Christian Gutenkunst is mainly responsible for the DrivingCube and the data evaluation. Christian Gutenkunst and Jonas Nesensohn enriched this paper with their research work. Tobias Düser, Bernhard Schick and Houssem Abdellatif made an essential contribution to the conception of the research project. They revised the paper critically for important intellectual content.

## REFERENCES

- [1] Matthias Stiller. “Absicherung von Systemen für das (hoch)automatisierte Fahren”. In: *6. AutoTest Fachkonferenz*. Stuttgart, 2016.
- [2] Hermann Winner and Walther Wachenfeld. “Absicherung automatischen Fahrens”. In: *6. FAS-Tagung*. Munich, 2013.
- [3] Economic Commission for Europe of the United Nations (UN/ECE). *Regulation No. 140 — Uniform provisions concerning the approval of passenger cars with regard to Electronic Stability Control (ESC) Systems*. 2017.
- [4] Tobias Düser. “X-in-the-Loop – an integrated validation framework for vehicle development using powertrain functions and driver assistance systems”. PhD thesis. Institut für Produktentwicklung (IPEK), Karlsruher Institut für Technologie (KIT), 2010.
- [5] Fabian Schuldt. “Ein Beitrag für den methodischen Test von automatisierten Fahrfunktionen mit Hilfe von virtuellen Umgebungen”. PhD thesis. TU Braunschweig, 2016, p. 67.
- [6] Hermann Winner et al., eds. *Handbuch Fahrerassistenzsysteme*. 3rd ed. ATZ/MTZ-Fachbuch. Wiesbaden: Springer Vieweg, 2015, pp. 76–83. ISBN: 978-3-658-05733-6.
- [7] Albert Lutz et al. “Simulation methods supporting homologation of Electronic Stability Control in vehicle variants”. In: *Vehicle System Dynamics* 55.10 (2017), pp. 1432–1497. ISSN: 0042-3114.
- [8] *Passenger cars – Vehicle dynamic simulation and validation – Steady-state circular driving behaviour*. ISO 19364:2016-10. International Organization for Standardization, 2016.
- [9] *Passenger cars – Steady-state circular driving behaviour – Open-loop test methods*. ISO 4138:2012. International Organization for Standardization, 2012.

- [10] *Passenger cars – Validation of vehicle dynamic simulation – Sine with dwell stability control testing*. ISO 19365:2016. International Organization for Standardization, 2016.
- [11] *Jahresbericht 2017*. DIN annual report. DIN-Normenausschuss Automobiltechnik (NAAutomobil), 2017.
- [12] Albert Albers and Tobias Düser. “Integration of Simulation and Test using Vehicle-in-loop technology at the roller test bench and in the road test”. In: 3. *Internationales Symposium für Entwicklungsmethodik*. Wiesbaden, 2009.
- [13] S. Metzner and H. Schreiber. “Radar stimulation for a novel ADAS system in-tegration platform”. In: *Grazer Symposium Virtual Vehicle 2017*. Graz, 2017.
- [14] *Road vehicles – Determination of centre of gravity*. ISO 10392:2011. International Organization for Standardization, 2011.
- [15] *Intelligent transport systems – Full speed range adaptive cruise control (FSRA) systems – Performance requirements and test procedures*. ISO 22179:2009. International Organization for Standardization, 2009.
- [16] *Road vehicles; vehicle dynamics and road-holding ability; vocabulary*. DIN 70000:1994-01. Deutsches Institut für Normung, 1994.
- [17] C. Schyr and A. Brissard. “DrivingCube - A novel concept for validation of powertrain and steering systems with automated driving”. In: *Proceedings of the 13th International Symposium on Advanced Vehicle Control (AVEC)*. Munich, 2016, pp. 79–84.
- [18] Economic Commission for Europe of the United Nations (UN/ECE). *Regulation No. 101 — Uniform provisions concerning the approval of passenger cars powered by an internal combustion engine only, or powered by a hybrid electric power train with regard to the measurement of the emission of carbon dioxide and fuel consumption and/or the measurement of electric energy consumption and electric range, and of categories M1 and N1 vehicles powered by an electric power train only with regard to the measurement of electric energy consumption and electric range*. 2012.